A review of laser scanning three-dimensional digitisers

Josep Forest and Joaquim Salvi

Institut d'informàtica i aplicacions
Universitat de Girona
Lluís Santaló s/n, 17071 - Girona (Catalunya)

Abstract

A big number of products are sold by their shape features, hence, process engineers are including more and more accurate 3D digitisers in their manufacturing assembly lines. Acquisition and data processing speed are becoming important issues to consider when choosing the right device to be incorporated in the inspection equipment without loss of accuracy. This paper is intended to present an exhaustive review of the state-of-the-art about laser scanning three-dimensional digitisers, proposing a classification of such systems.

1 Introduction

A three-dimensional digitiser is often called *range finder* too, stating its capability for acquiring **range** or *depth* information. These devices use to grab "range images", also called "$2\frac{1}{2}$D images", which are dense arrays of values related to the distance of the scene to a known point or plane.

Many laser scanning three-dimensional digitiser systems use one or more standard CCD cameras and scanning laser slits, and triangulation techniques are mostly used in the 3D reconstruction of the scenes. Some of these systems operate grabbing one image per each sweep step, so it is a time consuming process, yielding a big amount of images. However, using high speed vision modules, rates of up to 1.6 complete scans per second have been achieved. Speeds of up to 3 $2\frac{1}{2}$D images per second have been achieved using standard CCD cameras, though. The operation of such systems rely on the fast switching of the light source and the CCD shutter operation in order to get space-encoded images. Table 1 shows a small comparison of leading manufacturers[1] in terms of accuracy and acquisition speed.

Some research has been done by [9], [31] toward the development of *Smart sensors* capable of delivering up to 1000 $2\frac{1}{2}$D images per second, but only

---

[1]A complete list of manufacturers with links to their own web pages can be found in *http://www.3dlinks.com/hardware_scanners.cfm*

Table 1: Commercial devices in terms of accuracy.

Model	Acc.[μm]	Speed[pps]	Dist.[mm]
T-Scan	±30	10K	83
Hyscan45c	±25	10K	60
Surveyor PS	±12	15K	100
Scantech	±50		

laboratory prototypes were developed.

2 Proposed classification

Table 2 shows the reviewed three-dimensional digitisers, reporting the main features they exhibit. Representative authors for each system are referenced, and an identifier sketch of every system is shown. This table is intended as a fast reference for the readers.
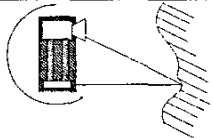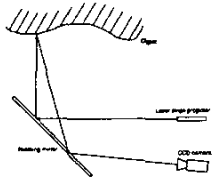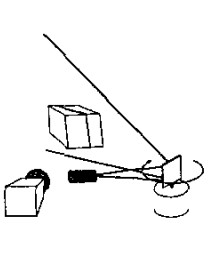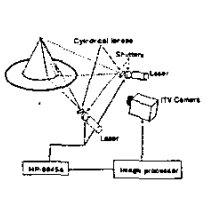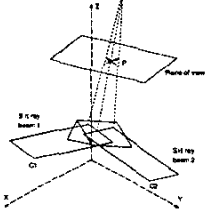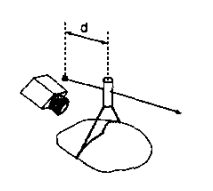
3 Systems and methods for shape acquisition

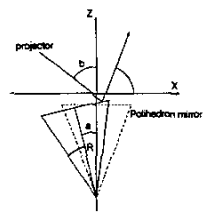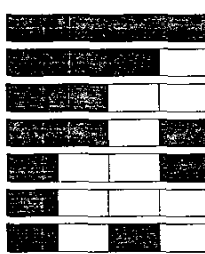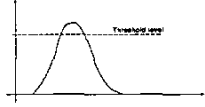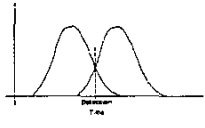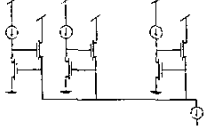This section discusses the methods surveyed in section 2, addressing the general description of each system according to the dissertation of the authors. It is structured into *Raw acquisition*, *Space-encoding* and *Smart sensors* subsections. A special attention is made on calibration and reconstruction issues.

3.1 Raw acquisition

By raw acquisition we mean that no encoding techniques have been applied to the process of acquiring a scene range map. That is, one image is captured by a frame grabber whenever a slit is projected onto the scene for a new position increment of the scanning mechanics. Hence, assuming the laser slit is vertical with respect to the image plane, n images are needed in order to get an n *column* range map. Shirai & Suwa [29] and Agin & Binford [1] used a video camera together with a plane-shaped laser light source projecting a slit onto a scene. The slit scanned the scene using a mirror attached to

Table 2: *Classification of three-dimensional digitisers, where:* **Sch.**→*Scheme,* **Auth**→*Author(s),* **Calib**→*Calibration procedure*

Sch.	Identifier	Features
R a w a c q u i s i t i o n		*Auth:*Chen & Kak [7] *Calib:*Projective geometry *Features:* • Single slit • Fixed geometry, rotates the whole system
		*Auth:*Reid [22] *Calib:*Projective geometry *Features:* • Single slit • Fixed geometry • Rotating mirror reflects both the image and laser slit
		*Auth:*Shirai et al.[29], Agin et al.[1], Popplestone[20] *Calib:* [29],[20] Accurate pose measurement of system devices [1] (A)-Camera calibration (B)- Estimation of laser slit position by image measurements *Features:* • Single slit • Rotating mirror reflects only the laser slit
		Auth: Sato[27] *Calib:* Point of light attached to the turntable at known radius and heights. *Features:* • Two slit projection • Turntable operation • Static laser and camera set • Minimisation of occlusions
		Auth: Nakano[19] *Calib:* Accurate pose measurement of system devices *Features:* • Two slit projection • Laser angular scanning • Eliminates reconstruction errors with lambertian surfaces
		*Auth:*Champleboux[5][6] *Calib:* (A) - Camera calibration using NPBS method. (B) - Accurate mechanical measurement and $R^3 \rightarrow R^3$ transformation identification *Features:* • Single slit • Linear scanning
S p a c e e n c o d i n g		*Auth:*Yu[33][32] *Calib:* Square pattern projection. System layout estimation using geometry analysis *Features:* • Single slit • Rotating mirror • Baseline error compensation • No special code was specified, although the system is versatile enough for adopting any codification • Compromise between acquisition speed and accuracy
		*Auth:*Sato[12][26][13] *Calib:* (A) - Camera calibration (Tsai [30]). (B) - Plane equation identification according to the space coding. *Features:* • Single slit • Rotating mirror • Compromise between acquisition speed and accuracy • Use of gray code in the pattern projection
S m a r t s e n s o r s		*Auth:* Gruss et al.[9][10], Kanade et al.[17], Hori et al.[14], Baba et al.[3] *Calib:* [9][10][17] Line-of-sight identification using a specially designed calibration target. The target is accurately positioned using a mechanical system *Features:* • Single slit • Rotating mirror • Cell-parallel architecture • Accuracy is determined by slit detection method • Slit detection using threshold on the illumination method
		Auth: K.Sato et al.[24], Yokohama et al.[31] *Calib:* Lookup table generation by finding the relationship between the scanning *time* and known depths. A plane is used as a calibration target *Features:* • Single slit • Rotating mirror • Cell-parallel architecture • Slit detection using comparison between two photosensitive areas in each cell
		Auth: Brajovic et al. [4] *Calib:* Acurate pose measurement. *Features:* • Single slit • Rotating mirror • Row-parallel architecture • Slit detection using one-per-row peak detectors • Slit detection using winner-take-all implementation ([18])

a stepper motor, and the camera was used for the acquisition of the slit images.

Chen & Kak [7] developed a similar three-dimensional digitiser, but the camera-projector set was arranged so that it formed a rigid structure, keeping their relative orientations invariant to each other.

Reid [22] used the same idea in order to provide the Oxford AGV with object recognition and acquisition capabilities. In this system, instead of making the device scan the scene itself, it is mounted on a static platform and a mirror is used in order to reflect both the laser stripe and the image. Experimental data is reported showing a 1% of error relative to the measured depths.

Calibration. Shirai & Suwa [29] calibrated their system by measuring the relative pose between the camera and the projector. Agin & Binford [1] used a calibration procedure consisting on a former camera calibration, followed by the estimation of the light projector position by grabbing a series of stripe images at known angular positions of the projector. A relaxation algorithm was used in order to minimise the position error.

Chen & Kak proposed a new calibration method based on the application of projective geometry. They stated that the points on the light plane could be mapped onto the image plane by finding the planar transformation (homography) which relates both planes. The reader is pointed to [8] or [11] to get deeper into projective geometry. The planes s and r correspond to the laser and image planes respectively. The calibration procedure is carried out with respect to a reference coordinate frame. A different coordinate frame F_s is associated to the laser plane which describes its pose with respect to the reference frame. A bi-dimensional coordinate frame F_{2s} is associated with the laser plane, where its axis x and y coincided with the axis x and y of F_s. This is an artifact used by the authors of [7] in order to easily change from the bi-dimensional coordinates of points on s to their corresponding three-dimensional representation.

Using the property of the cross-ratio invariance in projective space, one can define a 3x3 planar transformation mapping the points laying on a plane s into another plane r. Then, equation 1 is obtained, where ρ stands for the fact that in projective space, using homogeneous coordinates, every equation is defined up to a scale factor. The left hand side of this equation is the vector coordinate of a point laying on s (X_s), while the right hand side column vector describes the coordinates of a point laying on r (X_r). Arranging equation 1, considering

the geometrical transformations between frame coordinates, equation 2 is obtained, which maps a point on the image plane into its corresponding three dimensional point. The whole demonstration is described in detail in [7]. The matrix in equation 2 is called T_{cb}, or the *conversion matrix*.

From equation 2, x, y and z can be solved. Hence, a set of three linear equations is raised for every image point. Since ρ is a scale factor, the 4x3 matrix T_{cb} can be simplified fixing $t_{43} = 1$ without loss of generality. Hence, 11 unknowns (t_{11} to t_{33}) must be solved in order to complete the calibration process, so 4 coplanar non collinear points should be enough in order to solve for the system of equations. A system of 12 equations with 11 unknowns is raised, but as the points must be chosen such that they are coplanar, they must satisfy equation 3 too, which is *de facto* implicit in equation 2, meaning that the 12th equation is determined by the other 11. In practise, a set of more than 4 points is used, so an overdetermined system of equations is solved using a least square optimisation method. Experimental results made on a simple cubic object show that the relative accuracy of the system is dependent on the distance from the object to be scanned, obtaining errors of <0.05 inch at a distance of 20 inches and <0.04 inch at 14 inches, for the measure of the width, which is the side *perpendicular* to the optical axis of the camera. In addition, when the accuracy is evaluated measuring the height, which is the side *parallel* to the optical axis of the camera, the errors are one order of magnitude bigger, obtaining <0.30 inch at 20 inch and <0.14 inch at 14 inch.

$$\rho \cdot \begin{bmatrix} x_1 \\ x_2 \\ x_3 \end{bmatrix} = \begin{bmatrix} e_{11} & e_{12} & e_{13} \\ e_{21} & e_{22} & e_{23} \\ e_{31} & e_{32} & e_{33} \end{bmatrix} \cdot \begin{bmatrix} x'_1 \\ x'_2 \\ x'_3 \end{bmatrix} \quad (1)$$

$$\rho \cdot \begin{bmatrix} x \\ y \\ z \\ 1 \end{bmatrix} = \begin{bmatrix} t_{11} & t_{12} & t_{13} \\ t_{21} & t_{22} & t_{23} \\ t_{31} & t_{32} & t_{33} \\ t_{41} & t_{42} & t_{43} \end{bmatrix} \cdot \begin{bmatrix} u \\ v \\ 1 \end{bmatrix} \quad (2)$$

$$\det[X_b^1 X_b^2 X_b^3 X_b^4] = 0 \quad (3)$$

3.2 Space encoding. Switching the laser slit

Space-encoding stands for the projection of successive binary patterns onto the scene to be acquired. The number of patterns projected (n) is directly the number of bits used in the codification. Usually, the bright regions are assigned the logic level '1', and the dark regions are assigned a '0'. Finally, if each pattern is assigned a different weight, every pixel is

associated to a unique binary code, which can either be natural, gray or any suitable binary code. Space-encoding techniques are being applied using pattern projection ([21][16][15][23]). In these cases, the projector is modelled as a *reversed camera*. Sato et al. applied this technique in his *CubicScope* three-dimensional digitiser [28], using a scanning laser slit mechanism. The technique takes advantage of the shutter period of a standard CCD camera: within the time period in which the shutter is open, the laser slit must scan the scene in such a way that illuminated (bright) and shadowed (dark) regions appear. This technique requires the laser to be rapidly switched on and off. Due to the light integration given on the CCD, it stores a whole image as though a slide pattern was projected onto the scene. Hence, for each shutter period, a different pattern must be generated using the switching technique in order to get the proper patterned image, therefore, for n bit coding, n different patterns are required.

As an example of performance, consider the operation of a standard NTSC video camera that operates at 30 frames per second. Then, in order to achieve a rate of 1 $2\frac{1}{2}$D image in 0.3 seconds, a series of 9 patterns must be projected. This implies that a $2^9 - 1 = 511$ *columns* range map is obtained with 1% of accuracy. Yu et al. [33] used the space-encoding method on his laser scanning device. In this work, a study about the error introduced by the geometry of the polygonal mirror was reported (see table 2). In such arrangement, the rotating mirror has several different reflecting sides in order to achieve the optimal number of scans per motor turn. This makes the reflected slit to *effectively be projected* from somewhere away from the rotational axis, and this introduces an error in the calculation of the baseline B (ΔB_0). Equation 4 shows an equation for ΔB_0, deduced by [33]. A very thorough work on the estimation of calibration errors in laser scanning devices using space-encoding can be found in [32]. This work was done from the results published in [33].

$$\Delta B_0 = 2R \cdot (\cos a - \cos a_0) \cdot \frac{\sin(b - a)}{\cos(b - 2a)} \quad (4)$$

Calibration. Cubicscope [28] is calibrated in two steps: first, the CCD camera is calibrated using Tsai's method [30]. Second, regarding the scanning nature of the laser slit projection, each of the coded regions is assigned to a plane equation, hence, the second step of the calibration process is in charge of the accurate identification of every equation. In this sense, a mechanical arrangement consisting on an accurately positioned plane at different ranges from the digitiser is set up, then, on each of the planes a whole set of patterns is projected and the images

are stored. Every laser slit plane is identified by the equally coded regions imaged on each of the calibration planes, hence one laser slit plane equation is yeld for every coded region. In [13], a new approach using pattern shifting is tested with the aim of improving the accuracy at the expense of loosing acquisition speed. The pattern shifting method relies on the accurate detection of the regions' edges using the CCD charge storing effect.

In [32], Yu's digitiser is calibrated using a different method. The mechanical arrangement consists of a standardised plane, placed in front of the lens, within the view of the system, such that it is parallel to the xoy plane and perpendicular to the xoz. Using the switching technique for pattern generation, two concentric, different size squares are projected onto the calibration plane. Then, the plane is moved along the z axis until the biggest square fills the whole image plane, the calibration plane position is recorded, and the process is repeated for the smallest square. Using the known geometrical relation between the two squares, the different parameters are obtained. The reconstruction is done using triangulation and an accuracy of 1.5% is achieved.

3.3 Smart sensors. On-chip range computation

Using a timer instead of an external rotation sensor for acquiring angular position eliminates the need for an accurate position controller which drives the rotating mirror motor. Since with constant speed rotation, the scanning angle is proportional to the rotation speed, just a simple speed controller is required and hence the system hardware is notably simplified. Araki et al. [2] proposed a new method for measuring the *time* at which the slit image projects onto a photosensitive cell of a specifically designed discrete array. Each of the photosensitive cells has a timer register associated which is incremented until the image of the laser slit illuminates its associated photosensitive cell. Two optical switches are used in order to signal the start and the end of a scan period.

A simple threshold circuit was used in each cell in order to detect the light stripe image. The output of this circuit was used to stop the timer counting and store its value on the register itself. Once the light stripe mechanism fulfils a complete scan period, the register array is configured such that a big shift register is formed. Then the time values are transferred serially to the host computer.

A rotating mirror arrangement similar to that of [13] or [33] is used in this implementation.

Gruss et al. [9] proposed a VLSI version of a similar system. The difference with the system by [2] is that the time computation is made analogically,

using capacitor-based timing circuits, and a periodic sawtooth signal.

Analog time stamp recording is used instead of digital timers in order to avoid EMI from the switching clock signals to affect the photosensitive cells output. Kanade et al. [17] and [10] described a prototype implementation of the system in [9].

Yokohama et al. [31] and [25] proposed a new prototype similar to that of [9], incorporating notable improvements in slit detection. They used two side by side photosensitive areas in every cell, sensing the *difference* in light intensity between the two twin photo-diodes in every cell. The cell architecture uses three clock signals in order to set a 4-phase operation for synchronously sensing and transferring the data. A notable improvement in the accuracy has been achieved, obtaining a range error of $-24\mu m$ to $+14\mu m$, which is, in addition, very robust under the presence of significant levels of ambient light.

Calibration. In [10] the calibration target is a planar surface out of which a triangular section has been removed. This target is mounted on an accurate 3DOF[2] positioning device so its pose is accurately known. The calibration procedure is as follows: 1) the line-of-sight rays for a few cells are measured, and 2) a pinhole-camera model is fit to the measured line-of-sight straights in order to approximate the line-of-sight equation for all sensing elements.

The target is positioned so that its surface is parallel to the reference xy plane. Then the target is moved along the search path (see table 2 in Kanade's method) until an occlusion (the photosensitive cell does not detect the slit) occurs. Then, the 3D position of the target is recorded, and the process is repeated until both the bottom and top edges of the triangle are found. This procedure is made for different depths, so a set of *triangles* is recorded. The right corner of the triangle is found by calculating the bottom and top lines intersection for each of the triangles at the different depths. Finally, a line-of-sight equation is found by fitting a straight on the different corners found.

This calibration procedure is too slow to be applied to all the sensing elements, so in practise, a number of 25 evenly spaced of them are found. Finally, a least-squares procedure is used to fit a pinhole camera model. Experimental data for this system shows that for a range value within 0.5mm to 500mm, an accuracy of 0.1% is achieved. A transfer rate of 1,000 $2\frac{1}{2}$D images per second is achieved using this system. Yokohama et al. used a plane object for calibration. The procedure consists of 4 scans over the same plane, using 4 different depths. In each scan, the relationship between the scanning angle and the plane

depth is recorded for each photo-sensitive cell. At the end of the process, a lookup table is generated in order to allow for the real-time three-dimensional reconstruction.

4 Conclusions

There are no two identical calibration methods, but a different one exists for every different digitiser. Nevertheless, according to the nature of the hardware involved in each system, accuracy is always strongly dependent on the system calibration as well as the stripe detection accuracy. If video cameras are involved in the digitiser hardware, very accurate camera calibration methods have to be chosen according to the application specs and image distortion. In addition, the relative pose between the imager and the laser emitter must be carefully and accurately measured in order to get a proper shape measurement. Manual pose measurements are strongly disencouraged, since they induce very significant inaccuracies in the shape measurement. Accuracy and acquisition speed are the two main features one can expect to be as good as possible in a digitiser. Smart sensors offer very high speed rates and good accuracy. The methods based on standard cameras use to be much slower, although very high accuracies have been achieved.

References

[1] Gerald J. Agin and Thomas O. Binford. Computer description of curved objects. In *International Joint Conferences on Artificial Intelligence*, pages 629–640, 1973.

[2] Kazuo Araki, Yukio Sato, and Srinivasan Parthasarathy. High speed rangefinder. In SPIE, editor, *Optics, illumination and image sensing*, volume 850, pages 184–188, 1987.

[3] Mitsuru Baba, Tadataka Konishi, and Nobuaki Kobayashi. A new fast rangefinding method based on a non-mechanical scanning mechanism and a high-speed image sensor. In *IEEE Instrumentation and Measurement Technology Conference*, pages 957–962, 1997.

[4] Vladimir Brajovic, Kenichi Mori, and Nebojsa Jankovic. 100 frames/s cmos range image sensor. In *2001 IEEE International Solid State Conference*, pages 256,257 and 453, 2001.

[5] G. Champleboux, S. Lavallée, P. Sautout, and P. Cinquin. Accurate calibration of cameras and range imaging sensors: the npbs method. In *Proceedings of the 1992 IEEE International Conference on Robotics and Automation*, pages 1552–1557. IEEE, 1992.

[6] Guillaume Champleboux, Stéphane Lavalée, Richard Szelinski, and Lionel Brunie. From accurate imaging sensor calibration to accurate model-based 3-d object

---

[2]DOF:Degrees Of Freedom

localization. In *Proceedings of the IEEE Computer Vision and Pattern Recognition conference*, pages 83–89. IEEE, 1992.

[7] C.H. Chen and A.C. Kak. Modeling and calibration of a structured light scanner for 3-d robot viison. In *Proceedings of the IEEE conference on robotics and automation*, pages 807–815. IEEE, 1987.

[8] O. Faugeras. *Three-Dimensional Computer Vision: A Geometric Viewpoint.* The MIT Press, 1993.

[9] Andrew Gruss, Takeo Kanade, and L. Richard Carley. *Machine Vision for Three-Dimensional Scenes*, chapter A fast lightstripe rangefinding system with smart VLSI sensor, pages 381–397. Academic Press, Inc., 1990.

[10] Andrew Gruss, Shigeyuki Tada, and Takeo Kanade. A vlsi smart sensor for fast range imaging. In *Proceedings of the 1992 IEEE/RSJ International Conference on Intelligent Robots ans Systems*, pages 349–358, 1992.

[11] Richard Hartley and Andrew Zisserman. *Multiple view geometry.* Cambridge University Press, 2000.

[12] Kazuyuki Hattori and Yukio Sato. Handy rangefinder for active vision. In *Proceedings of the 1995 ieee international conference on robotics and automation*, pages 1423–1428, 1995.

[13] Kazuyuki Hattori and Yukio Sato. Accurate rangefinder with laser pattern shifting. In *Proceedings of the 1996 ieee international conference on robotics and automation*, pages 849–853, 1996.

[14] Yuko Hori, Mitsuru Baba, and Tadataka Konishi. A simultaneous high-speed measuring system of multiple points. In *IMTC'94*, pages 1365–1368, 1994.

[15] E. Horn and N. Kiryati. Toward optimal structured light patterns. *Image and Vision Computing*, 17(2):87–97, February 1999.

[16] S. Inokuchi, K. Sato, and F. Matsuda. Range imaging system for 3-D object recognition. In *Proceedings of the International Conference on Pattern Recognition*, pages 806–808, 1984.

[17] Takeo Kanade, A. Gruss, and L.R. Carley. A very fast vlsi rangefinder. In *Proc. IEEE International Conference on Robotics and Automation*, volume 2, pages 1322–1329, April 1991.

[18] J. Lazzaro, S. Ryckebusch, M.A. Mahowald, and C.A. Mead. Winner-take-all networks of o(n) complexity. In D.Tourestzky, editor, *Advances in Neural Information Processing Systems*, volume 1, pages 703–711, 1988.

[19] Kouichi Nakano, Yasuo Watanabe, and Sukeyasu Kanno. Extraction and recognition of 3-dimensional information by projecting a pair of slit-ray beams. In *Proceedings of the 9th International Conference on Pattern Recognition*, pages 736–743, 1988.

[20] R.J. Popplestone, C.M. Brown, and G.F. Crawford A.P. Ambler. Forming models of plane-and-cylinder faceted bodies from light stripes. In *International Joint Conferences on Artificial Intelligence*, pages 664–668, 1975.

[21] J. L. Posdamer and M. D. Altschuler. Surface measurement by space-encoded projected beam systems. *Computer Graphics and Image Processing*, 18(1):1–17, 1982.

[22] Ian D. Reid. Projective calibration of a laser-stripe range finder. *Image and Vision Computing*, (14):659–666, 1996.

[23] G. Sansoni, M. Carocci, and R. Rodella. Calibration and performance evaluation of a 3-D imaging sensor based on the projection of structured light. *IEEE Transactions on instrumentation and measurement*, 49(3):628–636, June 2000.

[24] Kosuke Sato, Atsushi Yokohama, and Seiji Inokuchi. Silicon range finder – a realtime range finding vlsi sensor –. In *IEEE 1994 Custom Integrated Circuits Conference*, pages 14.5.1–14.5.4, 1994.

[25] Kotsuke Sato, Atsushi Yokohama, and Seiji Inokuchi. Silicon range finder. In *Proceedings of the IEEE 1994 custom integrated circuits conference*, pages 339–342, 1994.

[26] Yukio Sato. Active rangefinding and recognition with cubicscope. In *Proceedings of the 2nd asian conference on computer vision*, pages 211–217, 1995.

[27] Yukio Sato, Hiroo Kitagawa, and Hiroichi Fujita. Shape measurement of curved objects using multiple slit-ray projections. *IEEE Transactions on Pattern Analysis and Machine Intellignece*, PAMI-4(6):641–646, 1982.

[28] Yukio Sato and Masaki Otsuki. Three-dimensional shape reconstruction by active rangefinder. In *Proceedings of the IEEE Computer Society Conference on Computer Vision and Pattern Recognition*, pages 142–147. IEEE, 1993.

[29] Yoshiaki Shirai and Motoi Suwa. Recognition of polyhedrons with a range finder. In *International Joint Conferences on Artificial Intelligence*, pages 80–87, 1971.

[30] R.Y. Tsai. *Synopsis of recent progress on camera calibration for 3D machine vision*, chapter The Robotic Review, pages 147–159. The MIT Press, 1986.

[31] A. Yokoyama, K. Sato, T. Yoshigahara, and S. Inokuchi. Realtime range imaging using adjustment-free photo-vlsi. In *Proceedings of the IEEE/RSJ International Conference on Intelligent Robots and Systems*, pages 1751–1758, 1994.

[32] Xiaoyang Yu, Jian Zhang, Liying Wu, and Qing Lin. Calibration errors in laser scanning 3d vision measurement using the space encoding method. In *Automated optical inspection*, volume 3558, pages 298–303. SPIE, 1998.

[33] Xiaoyang Yu, Jian Zhang, Liying Wu, and Xifu Qiang. Laser scanning device used ins space-encoding rangefinder. In *Automated optical inspection for industry*, pages 490–495. SPIE, 1996.